Available online at www.sciencedirect.com
SCIENCE DIRECT®
European Polymer Journal 41 (2005) 1380–1390
EUROPEAN POLYMER JOURNAL
www.elsevier.com/locate/europolj

Influence of a cooling rate on a structure of PA6

S.S. Pesetskii [a], B. Jurkowski [b,*], Y.A. Olkhov [c], S.P. Bogdanovich [a], V.N. Koval [a]

[a] *Laboratory of Chemical Technology of Polymeric Composite Materials, V.A., Belyi Metal-Polymer Research Institute of National Academy of Sciences of Belarus, 32a Kirov Street, 246050 Gomel, Belarus*
[b] *Institute of Material Technology, Poznan University of Technology, Piotrowo 3, 61-138 Poznan, Poland*
[c] *Institute of the Problems of Chemical Physics of Russian Academy of Sciences, 142432 Chernogolovka, Moscow Region, Russia*

Received 19 May 2004; received in revised form 11 December 2004; accepted 16 December 2004
Available online 10 February 2005

Abstract

The structure of the plate specimens obtained from the molten PA6 that was cooled at rates between 2 and 2000 °C/min have been studied. The cooling rate of 2000 °C/min did not ensure a complete amorphization of the specimens. The amorphous phase created by supercooling is unstable and at room temperature undergoes a noticeable cold crystallization. The access of water to the specimen from the surrounding air accelerates this process.

Variations in the cooling rate of the melt reflect in rearrangement of the amorphous phase of PA6. Owing to the effect of interaction with the crystalline phase, the amorphous regions undergo changes in molecular weight and MWD of the chain segments between junctions in topological regions, temperatures of the glass transition and β-relaxation, compaction, etc.

Keywords: Polyamide 6; Crystallization; Amorphous phase; WAXS; DSC; Relaxation spectrometry; TMA

1. Introduction

Amorphous and crystalline structures with different degree of order, packing density, and crystal perfection may be formed in PA6 [1–8]. This process depends on the conditions of cooling the melt, a presence of crystallization nuclei and plasticizers, mechanical stresses, electromagnetic fields, or other factors. Fast cooling may result in amorphous (or δ) structure [9–11] with density 1.097–1.10 g/cm^3 [12–14]. It is characterized by a low degree of ordering of the structural elements. The arrangement is mainly one-dimensional owing to low concentration of hydrogen bonds between –NH– and =CO groups in adjacent chains. A two-dimensional arrangement can be obtained in certain situations [9,15,16]. The transition from unstable structures into stable crystalline ones is studied extensively [2,10,15,17–20]. PA6 at supercooling of its melt develops a crystalline γ*-form that is unstable toward thermal exposure [2]. It could be transformed into a monoclinic one above 150 °C [4,16,17,21,22].

Polymorphic structures and their transformations in PA6 are usually studied by the X-ray technique [23]. In PA6 objects is observed a structure consisting an amorphous phase and the two crystalline forms. The

* Corresponding author. Tel.: +48 61 6652 776; fax: +48 61 6652 217.
E-mail address: boleslaw.jurkowski@put.poznan.pl (B. Jurkowski).

0014-3057/$ - see front matter © 2005 Elsevier Ltd. All rights reserved.
doi:10.1016/j.eurpolymj.2004.12.009

diffraction maxima of the different crystals and that of amorphous regions overlap because they are within the same range of $2\Theta = 15–20°$ angles. The amorphous portion is characterized by diffuse scattering only.

The information concerning the production of amorphous PA6, thermal and other conditions at which the material structure changes from amorphous to crystalline is rather contradictory. The nuclei of crystallization present in the melt prevent the structure from getting amorphous even at fast cooling rates. The nuclei could break down completely, but only during annealing the melt at 280 °C (the equilibrium melting point of PA6) for 90 min [11].

Supercooling of a thin layer of the melt makes it possible to produce a transparent film of PA6 [9] having an amorphous structure that is stable at room temperature. The film specimens heated at 110 °C for 3 h does not show any crystallization. When heated at 175–180 °C for 3 h, PA6 has crystallized fast and showed equilibrium of crystalline structures. According to another study [10], the chain segments in amorphous PA6 underwent ordering and nematic, smectic or pseudohexagonal (γ*) structures are formed when the material is heated up to 50 °C, i.e. to a temperature close to T_g.

The PA6 structures are usually studied on fiber or film specimens. Information on the structure of PA6 plates is limited [16,23]. The amorphous structural features of a plate of PA6 with different crystallinity degrees and perfection degree of the crystals have been studied inadequately. The technological capabilities of producing amorphous material as plates are not clear as well as the kinetics and thermal conditions necessary for changing δ-amorphous form to crystalline one. The aim of present work is to perform an analysis of structural changes, particularly referring to the amorphous phase, in PA6 plate specimens prepared from the melt that had been cooled at different rates.

2. Experimental

2.1. Materials

Polyamide 6 (PA6) was supplied by the Khimvolokno Company, Grodno, Belarus. The relative viscosity of the material in H_2SO_4 is 2.6; the melting point is 222 °C.

2.2. Specimen preparation

Test specimens were obtained from the melt ($T_m = 240$ °C) by injection molding in the laboratory machine of piston type (injection volume 3 cm^3). The cooling rate of PA6 melt was changed by varying the initial temperature of the mould. It was determined by using thermocouples to measure the temperature of the mould near its cavity that filled with the polymer. A slow cooling rate was about 2 °C/min; an intermediate one was about 100 °C/min. The fast cooling (at about 2000 °C/min) was conducted as follows: the metallic plates were cooled in liquid nitrogen; then molten PA6 in the form of jet that had been heated up to 240 °C was run between the steel plates having an initial temperature of about −100 °C. In this case, variations in the cooling rate within the specimen are possible. In central zone of the specimen where the thermocouples were now located, a quenching runs at the lowest rate due to the lowest heat transfer. Consequently, structural transformations there occur deeper than those in outer zones contacting a steel surface. Because of this, a cooling rate in central zone (about 2000 °C/min) is accepted as the main for the studied process.

For the cooling rates of 2 and 100 °C/min, the specimens for DSC and WAXS investigations were as strips 5 mm wide and 4 mm thick. For the relaxation measurements, test strips in a size of $50 \times 5 \times 1$ mm were used. In the case of cooling rate of 2000 °C/min, for all the tests, specimens in the form of plates of about 1 mm thick were cut with a punching die.

2.3. X-ray analysis

The X-ray analysis was performed by the WAXS method using the diffractometer DRON (Nauchpribor Co., Orlov, Russia) with CuK_α—radiation source ($\lambda = 0.1542$ nm) and Ni filter (slot 10 μm) (Cu anode, voltage 40 kV, current 30 mA). The diffractograms were recorded for angles (2Θ) between 10° and 30°.

2.4. DSC analysis

The structural changes in specimens were estimated with respect to thermal effects of melting and crystallization by differential scanning calorimetry (DSM-10M, Institute of Biological Instruments, Russian Academy of Sciences). The specimens as slices were cut from the central region of PA6 plates; the weight was 7 mg; the heating and cooling rates were 16 °C/min. The temperature was measured within the accuracy of ±0.2 °C. The crystallinity degree was evaluated from the melting (crystallization) heat of PA6. The working standard was In ($T_m = 156$ °C, $\Delta H_m = 28.45$ J/g) [24].

2.5. Relaxation measurements

The relaxation transitions were studied by dynamic-mechanical loss method using the reverse torsion pendulum device designed at MPRI NAS of Belarus [25]. The pendulum frequency was 1 Hz. The specimens were heated at the rate of 1.5 °C/min within temperature range from −150 up to 200 °C. The temperature measurement accuracy was ±0.1 °C.

2.6. Thermomechanical analysis (TMA)

The TMA measurements were made using the UIP-70M device [26]. A PA6 specimen was placed in the instrument thermo-cryo-chamber and cooled at the rate of 5 °C/min to a temperature of −100 °C. A quartz probe was lowered onto the cooled specimen. The axial load on the probe was 0.5 g. The linear deformation there should not exceed 5% of the radius of a probe tip R_o = 1 mm. The specimen was then heated at a rate of 5 °C/min up to the temperature of its flow. Simultaneous changes in temperature and linear deformation of the specimen were recorded. The methodology used is given elsewhere [26–32]. The temperature measurement accuracy in the TMA chamber is ±0.05 °C while that of deformation is ±50 nm.

The version of TMA used is based on a model network with physical and/or chemical junctions and testing a layer up to 0.5 mm thick of polymers in rigid and viscoelastic states, and on idea of a topological structure of polymers consisting of several regions differing in thermal expansion properties. These regions are combined with each other by passing chains that create a co-continuous network. The high-temperature amorphous and crystalline regions can act as branching junctions in the low-temperature region of the amorphous phase.

2.7. Density measurements

The density was determined by means of hydrostatic weighing in *n*-heptane.

3. Results and discussion

3.1. WAXS and gravimetrical analyses

An increase in the cooling rate from 100 to 2000 °C/min when producing PA6 specimens from the melt does not cause any qualitative changes in the diffractograms (Fig. 1). The curves have a distinct peak at angle $2\Theta = 21.4°$ that indicates a presence of a crystalline structure in the polymer.

At the cooling rate of 2 °C/min, a qualitative change occurs in the diffractograms. The presence of two peaks at sliding angle $2\Theta = 20.6°$ (crystal plane 200) and at $2\Theta = 24°$ (plane 002/202) points out that slow cooling makes it possible to crystallize PA6 and create a monoclinic structure [15,16]. The structures formed at cooling rates of 100 and 2000 °C/min should be termed as unstable γ*-form with a pseudo-hexagonal elementary cell [2].

The comparison of the crystallinity degree by areas under diffraction peaks for different crystal forms is disputable [16,18,23]. Because of this, the data of density measurements have been used for indirect evaluation

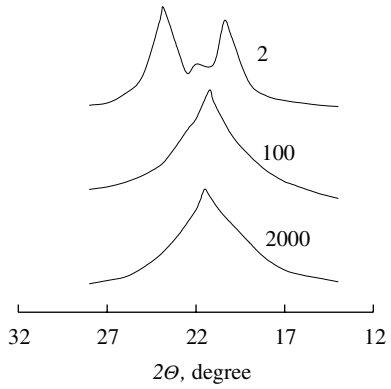

Fig. 1. Diffractograms (WAXS) of PA6: numbers on curves stand for cooling rates from the melt in °C/min.

of the trends in changes of the initial crystallinity degree. Polymer density for a cooling rate of 2000 °C/min was 1.092 g/cm^3, for 100 °C/min was 1.10 g/cm^3, and for 2 °C/min was 1.151 g/cm^3. It evidences that lower cooling rate is related to respective changes in the crystallinity degree. However, under experimental conditions, the specimen density for cooling rates of 100 and 2000 °C/min is close to that for amorphous PA6, which is 1.097–1.10 [12–14]. It seems worthless arguing about the absolute values for the crystallinity degree since the densities of different crystal forms differ from each other. Besides, the density of amorphous phase would vary with the degree of order [16,18,23].

Therefore, by increasing the cooling rate from 2 to 2000 °C/min for PA6 melt under the experimental conditions we failed to obtain entirely amorphous specimens (i.e., material with δ-structure only). At fast cooling (2000 °C/min) the specimens developed a structure with a low crystallinity degree and an unstable pseudo-hexagonal crystal structure (γ*-form).

3.2. DSC analysis

The specimens of the fast cooled melt underwent a cold crystallization in the measuring cell of the calorimeter (Tables 1 and 2 as well as Figs. 2 and 3). The temperature of the beginning of cold crystallization (T^*_{cr}) is 68.9 °C for specimen heated at 16 °C/min during DSC measurements. The temperature range within which the specimens undergo melting depends strongly on the cooling rate at which they were prepared, whereas the temperature range of crystallization remains unchanged (Table 1). The widest ΔT_m range is characteristic of fast-cooled specimens.

It may be assumed that dynamic heating of the fast-cooled PA6 results (owing to cold crystallization) in a mixture of structures having different symmetries of crystal forms [15] and melting temperatures that lead to a wider range of ΔT_m (Table 1).

Table 1
Parameters describing melting and crystallization of PA6 specimens prepared from the melt at different cooling rates

Parameter	Values versus cooling rate, °C/min		
	2000	100	2
T_m, °C	225	223	226
ΔT_m, °C	30	25	24.4
T_{cr}, °C	186	183	182
ΔT_{cr}, °C	18	18	18
ΔH_m, J/g	38.9	36.0	34.9
ΔH_{cr}, J/g	57.9	56.4	55.1

Table 2
Parameters describing melting and crystallization of PA6 specimens prepared from the melt at fast cooling (2000 °C/min) with exposure time in LDPE bag at 23 °C

Parameter	Annealing time, days					
	0	2	7	14	17	24
T_m, °C	225	224	224	225	224	225
ΔH_m, J/g	38.9	38.5	36.9	36.7	37.7	37.6
T_{cr}, °C	186	186	187	186	185	186
ΔH_{cr}, J/g	57.9	54.9	53.7	52.8	52.9	52.7
T^*_{cr}, °C	68.9	66.9	63.2	56.8	55.4	–
ΔH^*_{cr}, J/g	6.5	5.0	3.2	2.1	1.6	0

Note: ΔH_m, ΔH_{cr}, T_m, T_{cr} are heats and temperatures of melting and crystallization, respectively; ΔH^*_{cr}, T^*_{cr} are heat and temperature of cold crystallization.

The range of crystallization temperature for all specimens is the same, $\Delta T_c = 18$ °C (Table 1). However, the temperature of the beginning of crystallization for the specimens depends on a cooling rate. The highest $T_{cr} = 186$ °C is typical of fast-cooled specimens (Table 1) while the lowest (182 °C) is for PA6 cooled from the melt at a minimum rate. Since for DSC analysis all of the specimens were heated at similar conditions (up to 250 °C with isothermal exposure at this temperature for 1 min) it is believed that the cooling rate of the melt influences the stability of crystallization nuclei formed during subsequent melting of PA6. The most stable appear those nuclei that are found in the melt of the fast cooled polymer. Their presence explains the possibility of melt crystallization at 186 °C. Consequently, in view of the data from work [11] it can be assumed that "structural remembrance" of the PA6 melt depends not only on the thermal conditions of its treatment, but also on its initial modification (type of structure-forming nuclei).

The amorphous phase of fast-cooled PA6 is extremely unstable owing to cold crystallization (Table 2, Figs. 2 and 3). Its stability depends on the specimen storing conditions. After six days in the open air at ~23 °C, the cold crystallization of PA6 was completed. It is concluded from the lack of cold crystallization peak on DSC curve. The storage of specimens at limited access for humidity from air (if kept in a sealed LDPE bag) results in a longer time (up to 24 days) that was required for completing a cold crystallization (Table 2, Figs. 2 and 3).

The exposure of specimens at 2 °C in a refrigerator when they were sealed in a LDPE bag has shown that a cold crystallization would not complete during the test time (Fig. 3, curves 2 and 3). At −40 °C, no cold crystallization occurred according to DSC measurements (the crystallization heat did not change at storing, Fig. 3, curve 4).

Therefore, some mobility of PA6 chains causes that the amorphous phase, formed at fast cooling of the melt at favorable heat conditions, could transform in part into a non-equilibrium, but more thermodynamically stable, γ*-crystalline structure [15,16,23]. Evidently, the presence of amorphous and crystalline phases is most thermodynamically favorable for PA6 specimens in the form of plates.

A cold crystallization proceeds only under conditions of at least partially "unfrozen" mobility of PA6 chain segments (Fig. 3). For the fast-cooled specimens a range

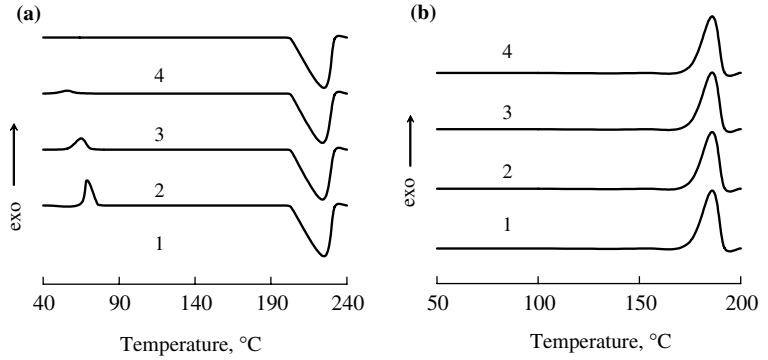

Fig. 2. DSC—heating (a) and cooling (b) curves for PA6 specimens prepared from the melt at 2000 °C/min cooling rate versus exposure time (days) in open air at 23 °C: (1) 0; (2) 1; (3) 3; (4) 6.

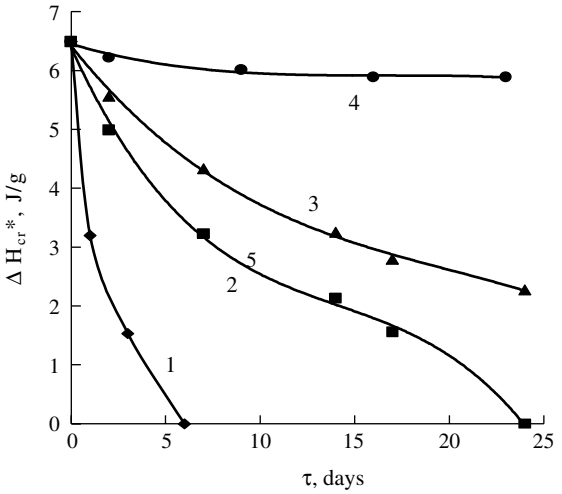

Fig. 3. Variations in cold crystallization heat for specimens prepared from the melt at 2000 °C/min cooling rate with exposure time (1) in open air at 23 °C; (2–4) in sealed LDPE bag at 23 °C (2); 2 °C (3); −40 °C (4), adequately.

of the glass transition temperatures for different structures is between −9 and 93 °C (Table 3). The exposure of specimens at −40 °C (at this temperature the mobility of structural units responsible for β-relaxation in PA6 is completely devitrified (Table 3)) does not lead to cold crystallization of the polymer (Fig. 3, curve 4).

Table 3
Temperatures of relaxation transition for PA6 specimens obtained at different cooling rates

Characteristic temperature for relaxation	Temperatures, °C for specimens cooled at rates, °C/min		
	2000	100	2
α-glass transition:			
T_{gb}	−9	−3	2
T_{g1}	33	38	29
T_g	43	46	54
T_{g2}	60	60	–
T_{gc}	93	112	121
ΔT_g	102	115	114
β-transition:			
$T_{\beta b}$	−91	−88	−87
T_β	−67	−62	−61
$T_{\beta c}$	−28	−24	−9
ΔT_β	63	64	78
γ-transition:			
T_γ	−135	−135	−135

Note: T_{gb}, T_{g1}, T_{g2}, T_g, T_{gc}, ΔT_g, $T_{\beta b}$, T_β, $T_{\beta c}$, ΔT_β, T_γ are, respectively, temperatures of the beginning of devitrification, kinks (T_{g1} and T_{g2}) on glass transition peak, glass-transition peak maximum, devitrification completion, temperature range for glass transition; beginning of β-process, its peak maximum completion and temperature range within which β-process occurs; peak maximum for γ-relaxation.

It is difficult to compare the changes in density mentioned in Section 3.1 with crystallization degree from DSC observations. It is because of substantial changes in crystallinity degree resulted from cold crystallization during DSC test due to the fact that a maximum crystallization rate of PA6 is observed at about 183 °C while the melting point is about 220 °C.

It can be presumed that variations in the cooling rate for PA6 melt would alter the structural and molecular characteristics of both the amorphous and crystalline phases. To determine such changes, the relaxation spectroscopy and TMA were used [18,27,33].

3.3. Relaxation properties

The variations in the cooling rate at which specimens are obtained influence the α- and β-relaxations in PA6, but do not virtually influence the γ-relaxation (Fig. 4 and Table 3). It should be noted that values for $\tan\delta$ and G' are only correct for specimens obtained at 2 and 100 °C/min cooling rates because the specimens obtained at 2000 °C/min showed variations in thickness that substantially influence the distribution of stresses within a specimen at testing. Therefore, in the latter case the calculated values of $\tan\delta$ and G' are tentative and cannot be used for a quantitative comparison with specimens obtained at lower cooling rates.

The α-relaxation in PA6 is caused by segmental motion of the chains [33]. The data in Fig. 4(a) and Table 3 show that the cooling rate affects not only the temperature-dependent location of the glass-transition peak, but also the character of relaxation events in the glass-transition region. As the glass transition in semi-crystalline polymers depends on segmental mobility in the amorphous phase only [33], it is evident that a cooling rate substantially influences the amorphous structure of PA6. A decrease in the cooling rate (material's crystallinity degree increases) causes T_g to rise from 43 to 54 °C (Table 3). The reason for this can be a restricted segmental mobility in the amorphous phase with an increased crystallinity degree of the material at the expense of interactions between chains. On the other hand, T_g of PA6 strongly depends on the amount of water absorbed by it [34]. It is because dry PA6 usually has $T_g \approx 50$–60 °C while that containing a maximum amount of water (around 11 wt.%) has $T_g = -40$ °C. The crystalline phase of PA6 contains no water [35]. Consequently, clusters of liquid water are only present in amorphous regions of the polymer.

All of the specimens had identical relative humidity (about 0.1%). Since fast-cooled specimens contain larger amounts of the amorphous phase then, with equal contents of water, its concentration in the amorphous

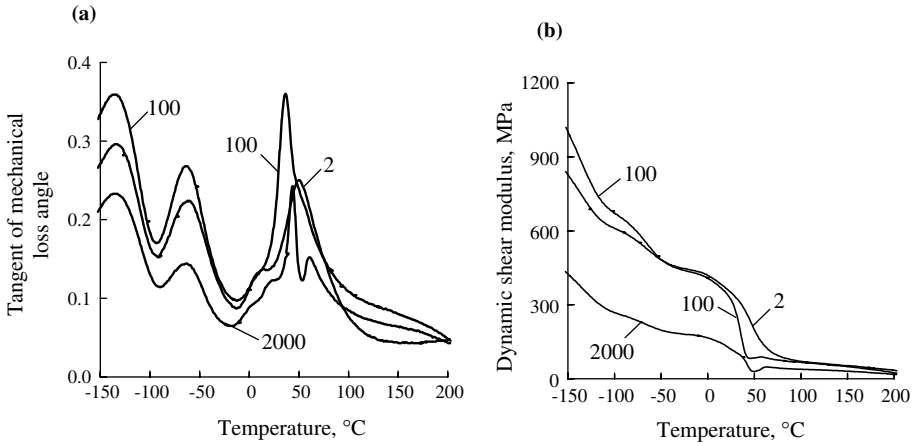

Fig. 4. Temperature dependences of (a) mechanical loss angle and (b) dynamic shear modulus for PA6. Numbers stand for cooling rates in °C/min.

regions must be lower than that in slowly cooled specimens. Consequently, the main reason for shifting T_g to the higher temperature at a decreased cooling rate is a restricted segmental mobility in the amorphous regions owing to interactions with the crystalline phase.

On the ascending arm of the glass-transition peak (on the low-temperature side) there is a kink at 33–38 °C for all of the specimens. This fact can be explained by the completion of the glass transition in less bound (i.e. more mobile) segments and the beginning of devitrification in the more ordered fraction of chain segments, the mobility of which is restricted by their interaction with crystals.

The higher-temperature arm of the glass-transition peak for specimens obtained at intermediate cooling rates shows a kink at 60 °C while for the fast-cooled specimens such kink transforms to a distinct peak of mechanical losses. The reason for this behavior is cold crystallization of PA6. After such crystallization occurs, an increase in the shear modulus is observed (Fig. 4(b)). This is proved by the fact that there is no peak on the $\tan\delta$ curve at about 60 °C for slowly cooled (and consequently more crystallized) specimens. It should be noted that the cold crystallization can be observed by the relaxation spectrometry for specimens produced from the melt at 100 °C/min cooling rate, but the DSC cannot detect it. This could be caused by inadequate sensitivity of the DSC applied and small weight of the material (7 mg) used in the analysis, or by other factors.

The process of α-relaxation covers rather a wide temperature range (ΔT_g = 102–115 °C, Table 3). On gradually increasing the temperature within this range, the mobility of still higher molecular weight (MW) segments of chains unfreezes (their mobility is usually restricted by intermolecular interactions including the crystalline part of the polymer). The higher the cooling rate of PA6 (lower concentration of the crystalline part in it), the lower is the temperature of the glass transition onset (T_{gb}) as well as its completion (T_{gc}), Table 3, Fig. 4(a). This suggests that interaction with the crystalline part influences the segmental mobility in the amorphous phase of PA6.

The β-relaxation is related to the mobility of smaller than Kuhn segment structural units (coordinated motions of $-CH_2-$ and amide groups within a monomer unit) [35] both in amorphous and crystalline phases. This process proceeds not so easily in the crystalline phase as in the amorphous one that takes place at higher temperature [33]. In the studied case, variations in T_β could be caused by the effect of a cooling rate on the crystallinity degree of PA6. An increase in the cooling rate at specimens' preparation is accompanied by a quite considerable shift of T_β to the lower-temperature region ($T_\beta = -67$ °C for the fast cooled and $T_\beta = -61$ °C for the slowly cooled specimens, Table 3).

The low-temperature γ-relaxation results from mobility of individual $-CH_2-$ groups along the chains [3]. In the investigated case, the stable temperature of γ-process ($T_\gamma = -135$ °C) indicates that the supermolecular arrangement does not influence the mobility of individual $-CH_2-$ groups in PA6 chains.

3.4. TMA

3.4.1. Molecular and topological structure of PA6 specimens obtained at fast (2000 °C/min) cooling rate from the melt

The TMA was conducted on specimens that had been kept in sealed LDPE bags for approximately a fortnight. The thermomechanical curve (TMC) of PA6 (Fig. 5, curve 1) is typical of an amorphous polymer with a structure having two topological regions. For

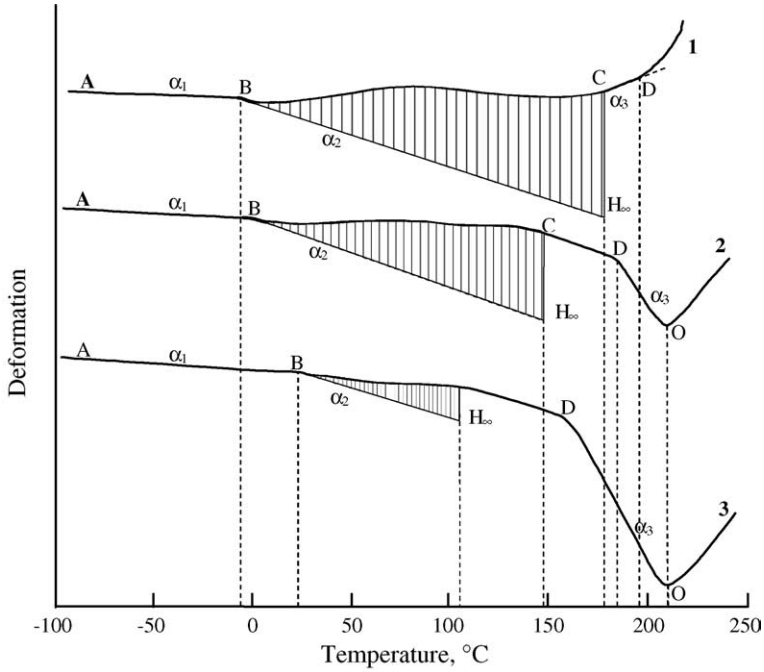

Fig. 5. Thermomechanical curves for PA6 specimens prepared from the melt at cooling rates, °C/min: (1) 2000; (2) 100; (3) 2, respectively.

the temperatures between −100 and −7 °C (the straight line segment AB) PA6 is in a glassy state and expands with temperature rising at a constant rate, and is characterized by the coefficient of linear thermal expansion $\alpha_1 = 4.41 \times 10^{-5}\ \mathrm{deg}^{-1}$ (Table 4). At the temperature corresponding to point B, the segmental mobility devitrifies ($T_g = -7$ °C) and the penetration deformation H_i starts to show with increasing temperature (shaded region) in the direction opposite to that of thermal expansion. This deformation results from a continuous development of the flow of chain segments from the shortest (Kuhn segment) to the higher MW ones at the temperature corresponding to point C (177 °C), and because of lower elastic modulus of the polymer [27–29]. It should be taken into consideration that each deformation H_i refers to the beginning of flow of PA6 chain segments between junctions in a pseudo-networked structure of its amorphous region of a particular molecular weight M_i. The following average MW were calculated for the chain segments: $\overline{M}_{a(n)} = 23.7$ kg/mol, $\overline{M}_{a(w)} = 37.9$ kg/mol (Table 4). Their MWD is shown in Fig. 6, curve 1. It is of three-modal nature that indicates a non-uniform distribution of the cluster-type branching junctions when a pseudo-network of the amorphous region is formed.

Beginning from $T_k = 177$ °C, related to point C on the TMC, deformation usually occurs owing to a change in the volume of voids including the free volume of the polymer amorphous region with a thermally stable pseudo-network [36–38]. As for PA6 specimens obtained at fast cooling from the melt, the plateau of high elasticity (CD straight line) is unusual in nature. On increasing the temperature, deformation grows at a constant rate (CD line) and has a negative coefficient of linear thermal expansion ($\alpha_3 = -29.8 \times 10^{-5}\ \mathrm{deg}^{-1}$). The share of topological branching junctions is 0.73 as calculated using the following empirical equation: $\varphi_T = 0.5–0.045(\alpha_3/\alpha_2 - 1)/P$ [32], where P is a load.

The abnormal deformation of the polymer over CD section of the TMC (Fig. 5, curve 1) can be explained by the presence of cluster-type branching junctions along with topological ones in the structure of the amorphous region as resulting from the entanglement of chain segments [38,39]. Their break down (relaxation) at increased temperatures would result in a lower elastic modulus of the material and deeper penetration of the TMA probe.

On the other hand, the abnormal deformation could be explained by a cold crystallization of the polymer that leads to a smaller specimen volume. Despite γ*-crystals present in the structure, no expansion characteristic of crystal melting was found in the TMC. It is evident from the TMA that γ*-form behaves in an unusual manner in comparison with crystalline and amorphous formations. The deformation behavior over CD section could be caused by a thermal relaxation of topological junctions.

Table 4
Properties of PA6 cooled from the melt at different rates (TMA measurements)*

Parameter, unit of measurement (95% confidence limit)	Cooling rate, °C/min		
	2000	100	2
Low-temperature amorphous region or soft amorphous fraction			
T_g, °C (±3–5)	−7	0	24
$\alpha_1 \times 10^5$, deg^{-1} (±10%)	4.41	5.47	5.89
$\alpha_2 \times 10^5$, deg^{-1} (±10%)	19.3	32.1	26.9
V_c^{TMA} (±10%)	0.119	0.213	0.177
$\overline{M}_{a(n)}$, kg/mol (±10%)	23.7	17.85	2.85
$\overline{M}_{a(w)}$, kg/mol (±10%)	37.9	27.2	4.1
K (±10%)	1.42	1.53	1.60
φ_a (±10%)	0.92	0.64	0.23
High-temperature amorphous region or rigid amorphous fraction			
T_k, °C (±3–5)	177	–	–
$\alpha_3(\alpha_{cr}) \times 10^5$, deg^{-1} (±10%)	−29.8	–	–
$\overline{M}_{cr(n)}$, kg/mol (±10%)	10.0	–	–
$\overline{M}_{cr(w)}$, kg/mol (±10%)	10.0	–	–
K_{cr} (±10%)	1.0	–	–
φ_{cr} (±10%)	0.08	–	–
φ_T (±10%)	0.55	–	–
T_f, °C (±3–5)	194	–	–
Crystalline region			
T_k (T_m), °C (±3–5)	–	182	154
$\alpha_3(\alpha_{cr}) \times 10^5$, deg^{-1} (±10%)	–	75.9	138.9
$\overline{M}_{cr(n)}$, kg/mol (±10%)	–	11.0	17.4
$\overline{M}_{cr(w)}$, kg/mol (±10%)	–	14.4	22.8
K_{cr} (±10%)	–	1.31	1.31
φ_{cr} (±10%)	–	0.36	0.77
T_f, °C (±3–5)	–	208	209
Molecular weight averaged over regions			
$\overline{M}_w$, kg/mol (±10%)	35.7	22.6	26.6

* *Note*: $K = \overline{M}_w/\overline{M}_n$—polydispersity index, $\overline{M}_w$—weight-average molecular weight, $\overline{M}_n$—number-average molecular weight, T_f—temperature of the beginning of molecular flow, T_g—glass transition temperature, T_m—temperature of the beginning of melting process, V_c^{TMA}—the fraction of voids = $3\Delta\alpha T_g$, $\Delta\alpha = \alpha_2 - \alpha_1$, α_1—coefficient of linear thermal expansion in a glassy state, α_2 is same as α_1 but in a high-elastic state, α_3—coefficient of linear thermal expansion during melting of a low-temperature crystalline portion, φ—weight share of the region, φ_T—share of topological junctions.

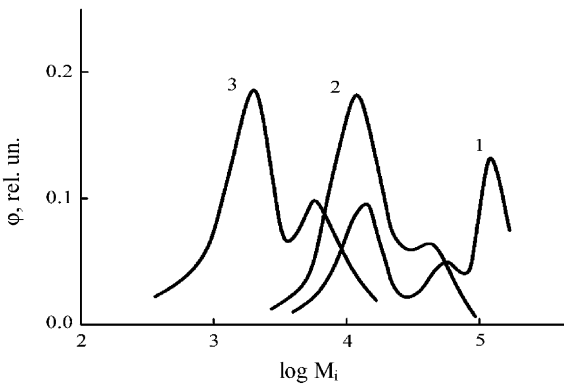

Fig. 6. MWD for chain segments between branching junctions in amorphous pseudo-networked region of PA6; specimens were prepared from the melt at cooling rates, °C/min: (1) 2000; (2) 100; (3) 2, respectively.

A cold crystallization of the amorphous PA6 could lead to γ*-form, which could be identified as ordered cluster-type structures.

The compaction factor calculated from the equation $V_c^{TMA} = 3(\alpha_2 - \alpha_1)T_g$ taken by analogy to the formula given in work [34], informs about the fraction of all voids present in the low-temperature region, it is 0.119. This value is related to PA6 chain mobility in this region and is comparable with that of rubbers.

The temperature T_k corresponding to point C on the TMC (Fig. 5, curve 1) that is related to approaching the CD plateau is to be taken as the temperature of relaxation onset in a cluster-type structure of the branching junctions in the high-temperature region; at this temperature, $V_c^{TMA} = 0.205$. Similar values of V_c^{TMA} are typical of rigid-chain polymers.

The lowest-MW chain segments of the high-temperature region can begin to flow at 194 °C (point D on

curve 1, Fig. 5) that coincides with the beginning of melting and molecular flow of PA6. The MW of these chain segments is $\overline{M}_n = \overline{M}_w = 0.65$ kg/mol. However, a polydispersive polymer at this temperature would not flow under the standard processing conditions. For proper processing, it requires a higher temperature to ensure a technological flow at a given shear rate, at which the highest MW polymer fractions start to flow. Because of this phenomenon, for a given polymer, the wider the MWD, the higher the processing temperature is.

3.4.2. Molecular and topological structure of PA6 specimens obtained from the melt at intermediate cooling rate (100 °C/min)

The TMC of PA6 for specimens obtained at a cooling rate of 100 °C/min (Fig. 5, curve 2) looks similar to that of a semi-crystalline polymer, the structure of which, within the temperature range from −100 to 250 °C, contains two topological regions: an amorphous pseudo-networked region and a crystalline one.

Within the temperature range from −100 to 0 °C, PA6 expands at a constant rate (AB line segment) characterized by coefficient $\alpha_1 = 5.47 \times 10^{-5}$ deg^{-1} (Table 4). At $T_g = 0$ °C, the segmental mobility in the amorphous region, starts to unfreeze, and a transition zone in TMC develops (BC section in curve 2, Fig. 5). The analysis gave averaged MW characteristics for the chain segments between junctions of a pseudo-network of the amorphous region: $\overline{M}_{a(n)} = 17.85$ kg/mol, $\overline{M}_{a(w)} = 27.2$ kg/mol, polydispersity index $K = 1.53$. The MWD for the chain segments between branching junctions (Fig. 6, curve 2) is bimodal which is indicative of more homogeneous (in comparison with PA6 specimen obtained at fast cooling) distribution of the cluster-type junctions of the pseudo-networked structure of the amorphous region.

At the temperature of point C ($T = 145$ °C), after segmental relaxation in the highest-MW homologue between junctions was completed, the polymer undergoes transition to a plateau (CD line) of high elastic deformation (Fig. 5, curve 2). Here, the pseudo-networked amorphous region expands, as was mentioned above, resulting from the increase in volume of voids, including the free volume, at the rate of $\alpha_2 = 32.1 \times 10^{-5}$ deg^{-1}. The value of $V_c^{TMA} = 0.213$ within the temperature range is found between C and D points.

Above the temperature corresponding to point D ($T_k = 182$ °C) the expansion rate of the polymer, being $\alpha_3 = 75.9 \times 10^{-5}$ deg^{-1} for DO interval, begins rising. The ratio of $\alpha_3/\alpha_1 = 13.88$ exceeds the critical value of 6.24 [38,40]. Therefore, the crystalline phase of the polymer undergoes melting within DO segment of the TMC (Fig. 5, curve 2). The MW of crystallized PA6 chain segments is proportional to $\Delta T = T_f - T_m$. For the highest-MW segment, it is 15.9 kg/mol, while for the lowest-MW homologue it is 10 kg/mol. The weight fractions of chain segments in topological regions (φ_a and φ_{cr}) are in direct proportion to the total deformation in each of them (H_∞ and H_k). Therefore $\varphi_\alpha = H_\infty/(H_\infty + H_k) = 0.64$ and $\varphi_{cr} = H_k/(H_\infty + H_k) = 0.36$.

The weight-average MW of PA6 averaged over the regions is $M_w = \overline{M}_{a(w)}\varphi_a + \overline{M}_{cr(w)} \times \varphi_{cr} = 22.6$ kg/mol.

Molten PA6 starts to flow molecularly at $T_f = 208$ °C (point O).

3.4.3. Molecular and topological structures of specimens obtained from slow-cooled (2 °C/min) PA6 melt

Fig. 5 (curve 3) represents a TMC and Fig. 6 (curve 3) represents the MWD for PA6 specimens cooled from the molten state at 2 °C/min. These curves are similar to those for specimen obtained from the melt that had been cooled at the intermediate rate. The topological structure of the former also has a semi-crystalline structure. It is evident from Table 4, however, that differences are present in all molecular, relaxation and other physical parameters including transition temperatures that characterize polymer properties. The share of the crystalline phase (Table 4) increases from 0.08 for fast-cooled specimens up to 0.77 for a minimal cooling rate (2 °C/min).

In view of the above we concluded that variations in the cooling rate influence not only the crystallinity degree of PA6, but also the relaxation parameters of the amorphous phase characterized by the MWD of the chain segments between junctions of its pseudo-network. In addition, the amorphous phase of PA6 plates prepared at different cooling rates is heterogeneous in composition as well as in mobility and relaxation behavior of its segments. Amorphous PA6 resulting from fast cooling shows a lower temperature of β-relaxation, which explains its higher freeze resistance.

4. Comparison of results obtained by different techniques

The analysis of the experimental data reported above shows a strong dependence of the structure and properties of PA6 amorphous phase on the structure of its crystalline part. It is not easy to obtain entirely amorphous specimens (with δ-structure only) by injection molding at the conditions described above. Since the temperature of devitrification is below 0 °C for the shortest chain segments (Kuhn segments) of amorphous polyamide, the material undergoes a cold crystallization at room temperature, and the presence of a crystalline phase in it can be detected by the WAXS and DSC techniques.

The thermodynamically unstable crystalline γ*-form, created by fast cooling from the melt in the case of its low content (up to 10%) in a polymer, can be identified by TMA as a cluster-type structure. As it was found from relaxation spectrometry, the change of γ*-form to

α-form of crystals with different packing density and increased crystallinity degree of PA6, causes substantial variations in the temperature of α- and β-relaxation transitions owing to cooperative motions of the chain segments and groups of atoms among monomer units, respectively. The reason for this is interaction between the amorphous phase and the crystalline part that influences not only the segmental mobility, but also the thermal motions of small-scale structural units responsible for β-relaxation in PA6. The kinks in the low-temperature region of the PA6 crystallization peak (Fig. 4(a)) are indicative of gradual devitrification of the segmental mobility of the amorphous phase having different interactions with the crystalline part. This devitrification process for specimens obtained at the cooling rate of 2 °C/min is completed at a maximum T_{gc} (121 °C). This temperature exceeds by 9–28 °C the T_{gc} of the specimens obtained at the cooling rates of 100 or 2000 °C/min. The unambiguous reason for this is a greater involvement of the amorphous phase in the interaction with the crystalline part as the latter concentration in PA6 gradually increases. The reason for the lack of information from TMA tests for the melting of crystals in the case under investigation is, most likely, their small concentration and their small size. The latter could be limiting for the case where the volume of crystals is comparable with the free volume of the polymer.

The crystallinity degree evaluated by TMA correlates with the changes in PA6 density. It should be noted that the initial crystallinity of PA6 is not easy to be determined by the DSC method in terms of the thermal effects of melting because of cold crystallization (pre-crystallization) that takes place during specimen heating.

5. Conclusions

An increase in the cooling rate of molten PA6 from 2 up to 2000 °C/min did not ensure a complete amorphization of the specimens tested. The amorphous phase (δ-structure) created at supercooling is unstable, and at room temperature it undergoes a cold crystallization. It could be presumed that water admission to a specimen from the surrounding air accelerates crystallization, but this conclusion should be confirmed by further studies. Cold crystallization does not occur at temperatures below that of devitrification onset for PA6 amorphous phase.

Variations in the cooling rate of the melt lead to polymorphous conversions in the crystalline phase (crystals with α-form are created at the cooling rate of 2 °C/min while the rates 100 and 2000 °C/min give crystals with predominantly unstable γ*-form) as well as to variations in the crystallinity degree and structural rearrangement in the amorphous phase. Owing to interactions with the crystalline phase, the amorphous phase may suffer alterations of the major parameters that describe their structure as well as service capabilities of a polymeric material such as MW and MWD of the chain segments between branching junctions in the pseudo-network of topological regions, temperatures of the glass-transition and β-relaxation, compactness, etc.

Information on the structure of PA6 studied by different methods is ambiguous. For example, the TMA technique is incapable of detecting the crystalline γ*-form.

Acknowledgement

The research was performed within the framework of the INTAS-03-55-2214 Project.

References

[1] Vogelsong DC. J Polym Sci 1963;A1:1055.
[2] Illers KH, Hoberkorn H, Simak P. Macromol Chem 1972; 158:285.
[3] Wallner LG. Monatsh Chem 1948;79:279.
[4] Holmes DR, Bunn CW, Smith DJ. J Polym Sci 1955; 17:159.
[5] Ziabicki A. Kolloid Z 1959;167:132.
[6] Ruscher DC, Gröbe V, Versäumer H. Faserforschung Textiltech 1961;12:214.
[7] Parker JP, Lindenmeyer PH. J Appl Polym Sci 1977; 21:821.
[8] Weyhe G, Pietzsch HR. Plaste Kautschuk 1993;40:73.
[9] Mikhailov NV, Klesman VO. Russian Kolloid J 1954; 26(23):191.
[10] Roldan G, Kaufman HS. J Polym Sci 1963;B1:603.
[11] Avramova N, Fakirov SI. Thirty third IUPAC Int Symp Macromol, Montreal, 1990. p. 374.
[12] Sandeman I, Keller A. J Polym Sci 1956;19:401.
[13] Bodor G, Holly Z, Kallo A. IUPAC Symp Macromol, Wiesbaden, 1959, presentation I-B-13.
[14] Rybnikar F. Chem Prumysl 1961;11:157.
[15] Strnad S, Malej S, Kreze T. Mat Rez Innovat 2002;5:243.
[16] Machulis AN, Tornau EE. Diffusive stability of polymers. Vilnius: Mintis; 1974 [in Russian].
[17] Samon JM, Schulz JM, Wu J, Hsioa B, Yeh F, Kolb R. J Polym Sci Phys 1999;37:1277.
[18] Wunderlich B. Prog Polym Sci 2003;28:383.
[19] Polo-Fritz L, Rosi V, Merani G. Faserforschung Textiltech 1972;23(8):359.
[20] Kinoshita Y. Macromol Chem 1959;33:1.
[21] Rybnikar F, Burda J. Faserforschung Textiltech 1961; 12(7):324.
[22] Gurato G, Frchera A, Grandi FZ, Zannetti R, Canal P. Macromol Chem 1974;175:953.
[23] Wunderlich B. Macromolecular physics V.1 crystal structure, morphology, defects. New York: Academic Press; 1973.
[24] Campoy I, Arribas JM, Zaporta MAM, Marco C, Gomez MA, Fatov JG. Eur Polym J 1995;31(N5):475.

[25] Pesetskii SS, Jurkowski B, Storozhuk IP, Koval VN J Appl Polym Sci 1999;73:1823.
[26] Jurkowska B, Olkhov YA, Jurkowski B. J Appl Polym Sci 1999;74(14):490.
[27] Olkhov YA, Baturin SM, Irzhak VI. Vysokomol Soed (Polym Sci) A 1996;38(5):849.
[28] Irzhak TF, Variukhin SE, Olkhov YA, Baturin SM, Irzhak VI. Vysokomol Soed (Polym Sci) A 1997;39(4):671.
[29] Olkhov YA, Irzhak VI. Vysokomol Soed (Polym Sci) 1998;406(10):1006.
[30] Olkhov YA, Irzhak VI, Baturin SM. RU Patent 1763952 A1 (27 Oct. 1989).
[31] Olkhov YA, Irzhak VI, Baturin SM. RU Patent 2023255 (27 Oct. 1989).
[32] Olkhov YA, Jurkowski B. J Therm Anal Cal, in press.
[33] Bartenev GM, Barteneva AG. Relaxation behavior of polymers. Moscow: Khimia; 1992 [in Russian].
[34] Simha R, Boyer RF. J Chem Phys 1962;37(5):1003.
[35] Lebedeva TV, Shapovalov SV, Plate NA. Vysokomol Soed (Polym Sci) 1996;38A-B(12):1986.
[36] Pesetskii SS, Jurkowski B, Olkhov YA, Olkhova OM, Storozhuk IP, Mozheiko YM. Eur Polym J 2001;37: 2187.
[37] Pesetskii SS, Jurkowski B, Krivoguz YM, Olkhov YA. J Appl Polym Sci 2001;81:3439.
[38] Olkhov YA, Jurkowski B. J Appl Polym Sci 1997;65:499.
[39] Jurkowska B, Olkhov YA, Jurkowski B. J Appl Polym Sci 1998;68:2159.
[40] Jurkowski B, Jurkowska B, Andrzejczak K. Polym Testing 2002;21(2):135.